Water-Soluble GdF_3 and GdF_3/LaF_3 Nanoparticles—Physical Characterization and NMR Relaxation Properties

F. Evanics,[†] P. R. Diamente,[‡] F. C. J. M. van Veggel,*[,‡] G. J. Stanisz,[§] and R. S. Prosser*[,†]

Department of Chemistry, University of Toronto, UTM, 3359 Mississauga Road North, Mississauga, Ontario, Canada L5L 1C6, Department of Chemistry, University of Victoria, Victoria, British Columbia, Canada V8W 3V6, and Sunnybrook and Women's College Health Sciences Centre and Medical Biophysics, University of Toronto, Toronto, Ontario, Canada M4N 3M5

Received October 18, 2005. Revised Manuscript Received March 16, 2006

Nanoparticles consisting of either a solid core of GdF_3 or an 80/20 mixture of GdF_3 and LaF_3 have been prepared for use as NMR and MRI relaxation agents. To obtain high aqueous solubilities, the particles were coated with either citrate (**cit**) groups (in the case of GdF_3 nanoparticles), giving the nanoparticle a negatively charged surface, or 2-aminoethyl phosphate (**AEP**) groups (in the case of GdF_3/LaF_3 = 80/20), giving the nanoparticle a positively charged surface at physiological pH. In the presence of the 80/20 GdF_3/LaF_3:**AEP**, the paramagnetic contribution to the water spin−lattice relaxation rate was observed to be 7.5 s^{-1} at a nanoparticle concentration of 9.0 nM (0.78 mg/mL, 25 °C, 600 MHz ^{1}H Larmor frequency). Similarly, paramagnetic rates of 10.5 s^{-1} were observed for water using the GdF_3:**cit** nanoparticles at a nanoparticle concentration of 0.55 nM (0.77 mg/mL, 25 °C, 600 MHz ^{1}H Larmor frequency). Relaxivity measurements confirmed the potential of the particles for applications as contrast agents at MRI imaging field strengths. T_1 and T_2 experiments of the GdF_3:**cit** revealed mass relaxivities of 7.4 ± 0.2 and 8.4 ± 0.2 s^{-1} $(mg/mL)^{-1}$, respectively, at 1.5 T, whereas identical measurements at 3.0 T revealed respective relaxivities of 8.8 ± 0.2 and 9.4 ± 0.2 s^{-1} $(mg/mL)^{-1}$. The relatively high mass relaxivities exhibited by the nanoparticles may also find uses in NMR studies in which spin−lattice relaxation times are prohibitively long, as in the case of highly deuterated proteins. Direct interaction with the protein can be minimized by the use of surface charges opposite to the net charge of the molecule, whereas the nanoparticles are easily removed by ultracentrifugation.

Introduction

Paramagnetic contrast agents are routinely used in magnetic resonance imaging (MRI), because relatively small quantities can safely be introduced (often intravenously or orally), resulting in significant spin−lattice relaxation (T_1) or spin−spin (T_2) effects in certain tissues. Differences in T_1 or T_2 effects in neighboring tissues give contrast in MRI images, particularly when pulse sequences are employed to exploit such local differences.[1] This paper introduces a new class of water-soluble paramagnetic agents consisting of GdF_3 and mixed LaF_3/GdF_3 nanoparticles. Their advantages in MRI applications include the following: (1) high solubility in a range of solvents, (2) high mass relaxivity, and (3) ease of surface modifications for specific imaging needs. Paramagnetic nanoparticles may also have a future role to play in NMR. In the proteomics era, minimizing the time required to perform the requisite NMR assignments and structure studies is key to progress. Such studies often require months of NMR time for protein molecular weights in excess of 30 kDa. Moreover, strategies aimed at streamlining studies of large proteins and macromolecular complexes include the use of higher magnetic fields and partial deuteration. Consequently, spin−lattice relaxation times (T_1) become inordinately long and sensitivity (or time) is compromised. Paramagnetic relaxation agents such as the above may be used to quench solvent T_1's without undue line broadening of protein resonances. If the T_1 of water is sufficiently low, a considerable reduction of ^{1}H relaxation times is expected to occur on the surface and even the interior of the protein through water exchange and spin-diffusion. A case can also be made for using relaxation agents in high throughput NMR, or tandem analytical flow-through techniques, which combine NMR with HPLC and mass spectrometry. Assuming multiple scans are required for obtaining sufficient sensitivity in the NMR analysis, a lowering of T_1 would translate into a direct savings of time, because NMR is frequently the bottleneck in such tandem methods. Here, our first measurements characterizing the physical properties of these nanoparticles, water relaxivity, and relaxation effects on a solubilized protein are presented. The results are discussed in terms of applications for both MRI and NMR.

Paramagnetic Relaxation Agents and MRI and NMR Contrast Agents. Gd^{3+} is an ideal paramagnetic relaxation agent because of its large magnetic moment and nanosecond time scale electronic relaxation time.[2] Simple Gd^{3+} chelates

* To whom correspondence should be addressed. E-mail: fvv@uvic.ca (F.C.J.M.v.V.); sprosser@utm.utoronto.ca (R.S.P.).
† University of Toronto.
‡ University of Victoria.
§ Sunnybrook and Women's College Health Sciences Centre and Medical Biophysics.

(1) Brown, M. A.; Semelka, R. C. *MRI: Basic Principles and Applications*; John Wiley and Sons: New York, 2003.
(2) Bertini, I.; Luchinat, C. *NMR of Paramagnetic Molecules in Biological Systems*; Benjamin/Cumming: Menlo Park, CA, 1991.

10.1021/cm052299w CCC: $33.50 © 2006 American Chemical Society
Published on Web 04/19/2006

such as EDTA, DTPA, or DOTA are routinely used as paramagnetic relaxation agents in NMR studies, although there are several shortcomings. First, the gadolinium ion will coordinate with negatively charged ligands of the chelate, with water, and to some extent, with regions of partial charge on proteins or materials of interest, thereby excessively shifting and broadening some resonances and obscuring assignments. Second, rapid tumbling of a small complex diminishes the effectiveness of the relaxation agent, because the correlation time, τ_{eff}, associated with paramagnetic relaxation is a function of the average tumbling time of the Gd^{3+}chelate, τ_c, and the electronic relaxation time of the paramagnet, T_{1e}, such that

$$1/\tau_{eff} = 1/\tau_c + 1/T_{1e} \quad (1)$$

A wide variety of slow-tumbling water-soluble complexes that bind several to many Gd^{3+} ions have been designed, primarily for purposes of obtaining enhanced bulk water relaxation in MRI applications. In this case, the Gd^{3+} complexes dramatically decrease bulk relaxation times and therefore T_1-weighted images may reveal a significantly increased signal in tissues with higher Gd^{3+} concentration, hence improving MRI contrast. Such complexes include zeolites,[3] micellar aggregates,[4] polyamino acids,[5] polysaccharides,[6] and dendrimers.[7,8] Many of these materials would be problematic as relaxation agents in high throughput NMR or NMR studies of proteins because of nonspecific binding between chelate and the molecule of interest and background signal from the agent. Furthermore, although the majority of NMR experiments in assignment studies may benefit from a relaxation agent, others such as long-range NOESY distance measurements or relayed experiments, which require long-lived coherences, may perform worse with the addition of relaxation agents. Consequently, it is imperative that the relaxation agent can reliably and rapidly be removed so that the molecule under study can easily be retrieved. Conversely, this property of contrast agent is beneficial from the standpoint of dynamic enhanced contrast MRI (DCE-MRI), because it allows one to monitor contrast-agent perfusion.

Basic Physical Features of the GdF_3 and GdF_3/LaF_3 Nanoparticles. Nanoparticles have found many uses in wide-ranging fields of materials chemistry, including catalysts, energy storage, packaging and textiles, and advanced computing. In the health science industry, nanoparticles are used both as detection and delivery agents. For example, hydrophobic antitumor drugs can be packaged within nanoparticle matrixes, which commonly take the form of inorganic or organic polymers,[9] proteins or antibodies,[10] dendrimers,[11] or liposomes.[12] In some cases, the nanoparticle may be functionalized for targeting to a specific tissue or cell by additional ligation, and coatings such as lipopolysaccharides are frequently added to control drug release, endosomal uptake, and bioactivity. In this study, we present results of physical characterizations and NMR relaxation studies of solubilized nanoparticles consisting of either a solid core of GdF_3 or an 80/20 mixture of GdF_3 and LaF_3. High aqueous solubilities were achieved by coating the particles with either citrate groups (i.e., GdF_3:**cit** particles), resulting in negatively charged surfaces, or 2-aminoethyl phosphate groups (i.e., 80/20 GdF_3/LaF_3:**AEP**), resulting in positively charged surfaces at physiological pH. Basic NMR relaxation properties of nanoparticle-doped water as a function of temperature and field strength are presented and discussed, in addition to an analysis of corresponding relaxation behavior of a protein (lysozyme). Because of their high solubility and relaxivity, low background ^1H NMR signal, capacity to be functionalized with positive or negative surface charges, and ease of removal, and ability to be recovered from the supernatant (vide infra), the Gd^{3+}-rich fluoride nanoparticles should be useful as relaxation and contrast agents in NMR and MRI. To the best of our knowledge, the use of water-soluble GdF_3 and related nanoparticles has not been reported.

LaF_3 nanoparticles were introduced relatively recently,[13] and have shown promise for the telecommunications industry primarily because doping with Er^{3+}, Nd^{3+}, or Ho^{3+} confers unique luminescence properties in the regime where transmission is maximal for silica-based optical fibers (i.e., 1300−1600 nm).[14] Moreover, if the nanoparticle dimensions are on the order of a few nanometers, (Rayleigh) scattering will be negligible in polymer films. Finally, the inorganic LaF_3 matrix serves to shield the lanthanide ions from organic surroundings, thereby extending luminescence lifetimes. The synthesis of LaF_3 nanoparticles traditionally involved high-temperature conditions.[13] However, this procedure was later modified to allow for the formation of organic ligands on the nanoparticle exterior.[15] This step is key to rendering nanoparticles with high solubilities in organic solvents, thereby having the means to disperse the nanoparticles in polymer films for optical purposes. Fortunately, the synthesis protocol, discussed below, is sufficiently robust that functionalizing the surface for purposes of controlling solubility in a range of solvents is straightforward and indeed key to future MRI and NMR applications.[16]

Materials and Methods

Synthesis. *GdF_3 Stabilized with Citrates (GdF_3:**cit**).* A solution of citric acid (0.41 g, 2.13 mmol) in 25 mL of water was neutralized with $NH_4OH_{(aq)}$, followed by the addition of NaF (0.13 g, 3.00

(3) Young, S. W.; Qing, F.; Rubin, D.; Balkus, K. J.; Engel, J. S.; Lang, J.; Dow, W. C.; Mutch, J. D.; Miller, R. A. *Magn. Reson. Imag.* **1995**, *5*, 499.
(4) Andre, J. P.; Toth, E.; Fischer, H.; Seelig, A.; Macke, H. R.; Merbach, A. E. *Chem.—Eur. J.* **1999**, *5*, 2977.
(5) Aime, S.; Botta, M.; Garino, E.; Crich, S. G.; Giovenzana, G.; Pagliarin, R.; Palmisano, G.; Sisti, M. *Magn. Reson. Med.* **2000**, *6*, 2609.
(6) Lu, Z. R.; Parker, D. L.; Goodrich, K. C.; Wang, X. H.; Dalle, J. G.; Buswell, H. R. *Magn. Reson. Med.* **2004**, *51*, 27.
(7) Wiener, E. C.; Brechbiel, M. W.; Brothers, H.; Magin, R. L.; Gansow, O. A.; Tomalia, D. A.; Lauterbur, P. C. *Magn. Res. Med.* **1994**, *31*, 1.
(8) Yan, G. P.; Bottle, S. E.; Zhuo, R. X.; Wei, L.; Liu, M. L.; Li, L. Y. *J. Bioact. Compat. Polym.* **2004**, *19*, 453.
(9) Feng, S. S.; Mu, L.; Win, K. Y.; Huang, G. F. *Curr. Med. Chem.* **2004**, *11*, 413.
(10) Cloninger, M. *Drug Discovery Today* **2004**, *9*, 111.
(11) Gillies, E. R.; Frechet, J. M. J. *Drug Discovery Today* **2005**, *10*, 35.
(12) Feng, S. S.; Ruan, G.; Li, Q. T. *Biomaterials* **2004**, *25*, 5181.
(13) Zhou, J.; Wu, Z.; Zhang, Z.; Liu, W.; Dang, H. *Wear* **2001**, *249*, 333.
(14) Digonnet, M. J. F. *Rare Earth-Doped Fiber Lasers and Amplifiers*; Dekker: New York, 1993.
(15) Stouwdam, J. W.; van Veggel, F. C. J. M. *Nano Lett.* **2002**, *2*, 733.

mmol). The solution was heated to 75 °C followed by the addition of $Gd(NO_3)_3 \cdot 6H_2O$ (0.60 g, 1.33 mmol) in 2 mL of water. The 2 mL solution was added dropwise and stirred at 75 °C for 3−4 h, yielding a clear solution. Isolation of the particles was done by removing the water until the product was reduced to a pastelike consistency. Particles were redissolved in 5 mL of water and precipitated with ∼ 100 mL of ethanol. The particles were then isolated by centrifugation, after which the supernatant was poured off. The remaining precipitate was triturated with ethanol, separated by centrifugation, and dried under reduced pressure.

*GdF_3/LaF_3 (80/20) Stabilized with 2-Aminoethyl Phosphate (80/20 GdF_3/LaF_3:**AEP**).* A solution of 2-aminoethyl phosphate (0.14 g, 1.02 mmol) in 25 mL of water was neutralized with $NH_4OH_{(aq)}$, followed by the addition of NaF (0.13 g, 3.00 mmol). The solution was heated to 75 °C followed by the addition of $La(NO_3)_3 \cdot 6H_2O$ (0.12 g, 0.27 mmol) and $Gd(NO_3)_3 \cdot 6H_2O$ (0.48 g, 1.06 mmol) in 2 mL of water. The 2 mL solution was added dropwise and stirred at 75 °C for 3−4 h, yielding a clear solution. Isolation of the particles was achieved by removing the water until the product was reduced to a pastelike consistency, upon which the paste was redissolved in 5 mL of water and precipitated with ∼ 50 mL of acetone. The particles were isolated by centrifugation, after which the supernatant was poured off. The remaining precipitate was then triturated with acetone, separated by centrifugation, and dried under reduced pressure.

Characterization of the Nanoparticles. Atomic force microscopy (AFM) was done using a Thermomicroscope Explorer in contact mode, with a silicon nitride cantilever (0.01−0.5 N/m). The set point was estimated to be −7 nA at 1000 lines resolution, and the PID settings were 1.0, 0.5, and 0. Samples were deposited from a water suspension on a freshly cleaved mica substrate, in which the bulk of the water was subsequently desorbed via a piece of paper towel at the corner of the mica sheet. The particle size distribution was determined on the basis of a minimum of 150 particles. Dynamic light-scattering (DLS) experiments were carried out on a Brookhaven Instruments photon correlation spectrometer equipped with a BI-200SM goniometer, a BI-9000AT digital autocorrelator, and a Melles Griot He−Ne Laser (632.8 nm) with a maximum power output of 75 mW. All water and NP solutions were filtered through 0.45 μm Teflon syringe filters. Sample vials used for measurements were rinsed three times with the above filtered water. The final sample concentration used was 0.5 mg/mL. DLS experiments were performed at a 90° incident angle. The DLS measurements were done in triplicate on one batch for both the citrate- and AEP-stabilized nanoparticles. The extent of surface charge was also explored via zeta potential measurements using a Malvern Zetasizer (Malvern, U.K.). Energy-dispersive X-ray (EDX) analysis was done using a Hitachi S-3500N scanning electron microscope, operated at 20 kV and a resolution of 102 eV. Using concentrations comparable to those used in NMR experiments (i.e., 0.5 mg/mL), we determined the average zeta potential of the GdF_3:**cit** nanoparticles to be −2.4 ± 0.5 mV, suggesting that the nanoparticles form a stable dispersion. Solubilities were observed to improve considerably in the presence of even modest (25 mM) concentrations of salt (NaCl) or pH 6−7 buffer, which is most relevant to NMR. Moreover, under low salt concentrations, nanoparticle dispersions were observed to be stable for periods of months. Though not necessary for spectroscopic or imaging studies, 0.1 M concentrations were usually attainable. Similar zeta potential measurements were performed for the 80/20 GdF_3/LaF_3:**AEP** nanoparticles, where an average potential of 59.6 ± 2 mV was observed. Recent zeta potential measurements have been made on AEP-coated lanthanide-doped apatite calcium phosphate particles, for which zeta potentials on the order of +27 mV were observed.[17] Our AEP nanoparticles displayed excellent solubility and stability over periods of months in the presence of a small amount of buffer or salt (20 mM).

NMR Measurements. NMR experiments were performed on a 600 MHz Varian Inova spectrometer and a standard HCN liquids probe. Additional water T_1 measurements were performed on in-house 500 and 200 MHz NMR instruments, whereas low-field studies (1.5 T or 63.5 MHz and 3.0 T or 127 MHz) were measured using GE clinical imaging systems (GE, Signa). In NMR experiments at high fields, because of radiation damping effects, T_1 measurements of water were performed by employing a saturation and gradient pulse in place of the usual inversion pulse (i.e., a saturation recovery experiment). T_2 measurements were performed via a Carr Purcell Meiboom Gill (CPMG) pulse sequence with a refocusing delay of 2 ms. T_1 measurements at 1.5 and 3 T were performed using a standard inversion recovery spin−echo sequence with a repetition time (T_R) of 3000 ms, an echo time (T_E) of 7ms and eight inversion recovery times (T_I = 50, 100, 200, 300, 500, 700, 900, and 1500 ms). The field of view was 12 cm and the image plane was 128 × 128, slice thickness 3 mm; this allowed for simultaneous imaging of 12 vials containing 0.5 mL of different contrast agent concentrations. The regions of interest were then drawn for each of the vials at T_I = 1500 ms, and the signal containing on average 20 voxels for all T_I values was then evaluated. The signal-to-noise ratio was approximately 400. A CPMG imaging sequence with T_R/T_E = 2500/10 was used. The number of echoes collected was 96 and the number of averages = 4. Spectral analysis and peak deconvolution were performed using Varian software. In cases in which water suppression was necessary, a WATERGATE[18] sequence was generally employed. Lyophilized chick egg white lysozyme was obtained from Sigma Chemicals (Mississauga, ON) and used in a 100 mM pH 7 HEPES buffer for measurements of NMR spectra. Nanoparticles were added to the NMR sample(s) as a concentrated aqueous solution. Note that because phosphate buffer has been observed to cause precipitation of the GdF_3 nanoparticles on occasion, it should in general be avoided. NMR relaxivity measurements were also useful for correlating synthesis batches. The relaxivity profile from two separate batches was found to be identical within error at 600 MHz.

Separation of Nanoparticles. To remove the nanoparticles, the NMR sample was transferred to a 1.5 mL polycarbonate centrifuge tube, which was subsequently spun at 90 000 rpm for 45 min using a Beckman TL-100 ultracentrifuge and a TLA-100.2 fixed-angle rotor. The relative centrifugal force (RCF) at such speeds is estimated to generate an average of 288 489 times the force of the gravitational constant. After two such centrifugation cycles at 20 °C, a translucent gel was observed at the bottom of the tube, and the supernatant, including the solute molecules of interest, could easily be extracted. A second method of separation could be implemented using beads or affinity columns consisting of avidin. In this case, upon biotinylation, nanoparticles may easily be removed from the solution. Studies were also performed to estimate

(16) (a) Sivakumar, S.; van Veggel, F. C. J. M.; Raudsepp, M. *J. Am. Chem. Soc.* **2005**, *127*, 12464. (b) Sudarsan, V.; Sivakumar, S.; van Veggel, F. C. J. M.; Raudsepp, M. *Chem. Mater.* **2005**, *17*, 4736. (c) Stouwdam, J. W.; Raudsepp, M.; van Veggel, F. C. J. M. *Langmuir* **2005**, *21*, 7003. (d) V. Sudarsan; van Veggel, F. C. J. M.; Herring, R. A.; Raudsepp, M. *J. Mater. Chem.* **2005**, *15*, 1332. (e) Dekker, R.; Klunder, D. J. W.; Borreman, A.; Diemeer, M. B. J.; Worhoff, K.; Driessen, A.; Stouwdam, J. W.; van Veggel, F. C. J. M. *Appl. Phys. Lett.* **2004**, *85*, 6104. (f) Stouwdam, J. W.; van Veggel, F. C. J. M. *Langmuir* **2004**, *20*, 11763.

(17) Lebugle, A.; Pelle, F.; Charvillat, C.; Rousselot, I.; Chane-Ching, J. Y. *Chem. Commun.* **2006**, 606.

(18) Piotto, M.; Saudek, V.; Sklenar, V. *J. Biomol. NMR* **1992**, 661.

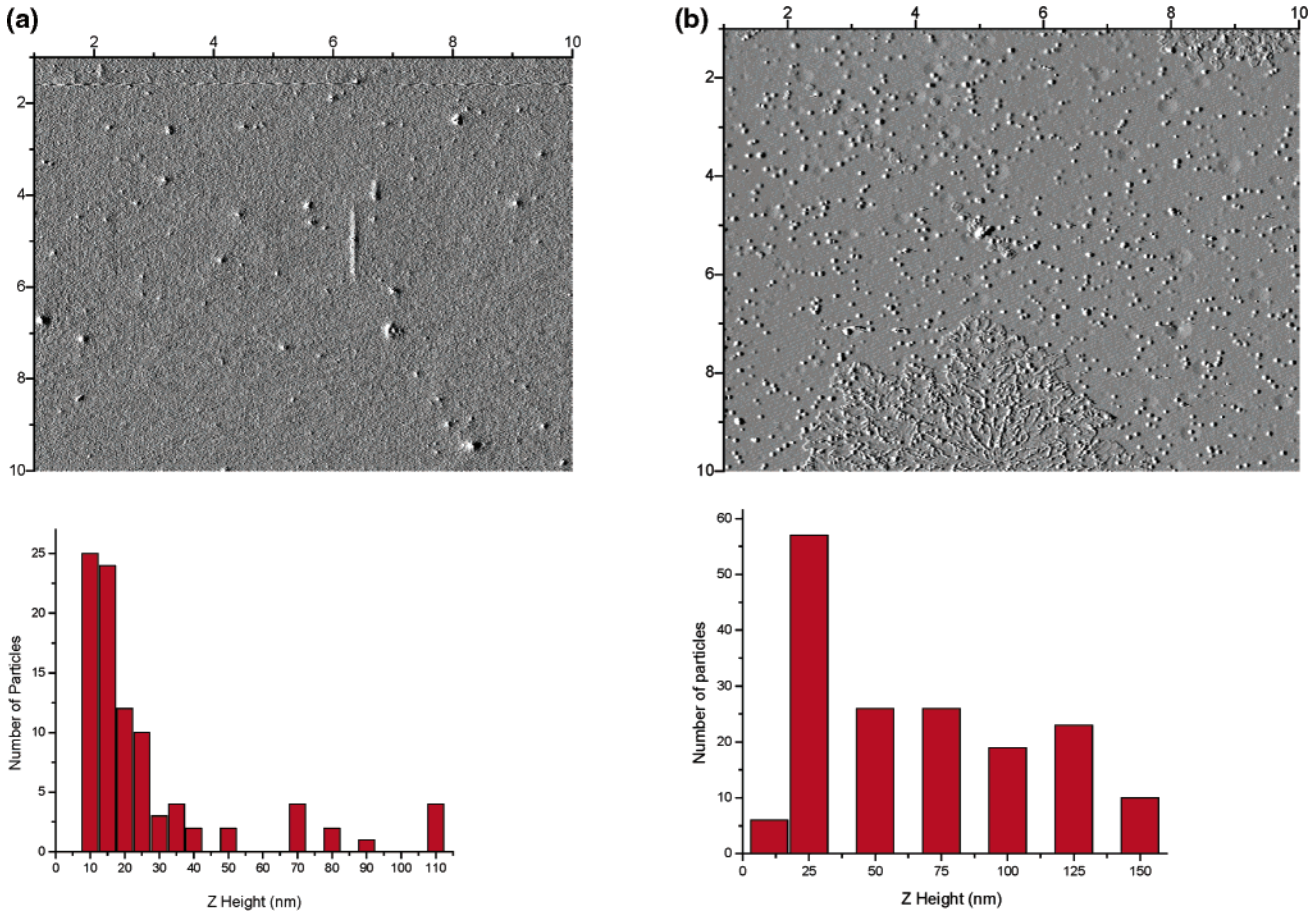

Figure 1. Atomic force microscopy images of nanoparticles, consisting of (a) an 80/20 mixture of GdF_3 and LaF_3, surface functionalized with aminoethyl phosphate, and (b) GdF_3, surface functionalized with citrate. The histograms in each system reveal a broad distribution of particle sizes, consistent with typical cross-sectional diameters of 51.5 nm for the 80/20 GdF_3/LaF_3:**AEP** particles and 129.3 nm for the GdF_3:**cit** particles, as determined by dynamic light-scattering measurements.

the extent of leaching. Upon separation of the particles by ultracentrifugation, the supernatant was extracted either immediately, or after 1 and 3 days. In all cases, no Gd^{3+} ions could be detected in the supernatant, as judged by water relaxation times, which remained perfectly constant in the 90/10 $H_2O/^2H_2O$ system, suggesting that leaching is either extremely slow or nonexistent. This suggests that toxicity is probably low, which is supported by a study by Palmer et al. that shows the LD_{50} of lanthanide oxides is 1000 mg/kg.[19] Size control to around 20 nm also allows for the reduction of the retention time in the body.[20] More recently, studies of ^{15}N-enriched Fyn SH3 protein upon centrifugation of the nanoparticles and extraction of the supernatant reveal absolutely no change in line width or frequency of any amide resonances, also suggesting no free Gd^{3+} ions. It is important to use nanoparticles with a charge opposite to that of the protein to avoid precipitation.

Results and Discussion

The GdF_3:**cit** and 80/20 GdF_3/LaF_3:**AEP** nanoparticle morphologies and sizes were characterized by dynamic light scattering (DLS) and atomic force microscopy (AFM). Panels a and b of Figure 1, obtained from atomic force microscopy, reveal broad distributions of particle sizes for both classes of nanoparticles. In the case of the $GdF_3:LaF_3$:**AEP** nanoparticles, atomic force measurements reveal a roughly bimodal size distribution with particle cross sections ranging from 10 to 50 and 80 to 110 nm, although sizes between 30 and 60 nm are more typical. The larger particles, in this case, are not suspected to consist of agglomerated particles from the 10−50 nm dimensions. An analysis of dynamic light-scattering measurements corroborates the size range estimated by AFM and suggests an effective diameter of 51.5 nm in H_2O (average of 3 measurements), with an experimental error of 5 nm and a size range matching that of the AFM distribution. To support this further, we performed DLS measurements on samples taken from the reaction mixture, i.e., before the precipitation step, which gave essentially the same size distribution as the isolated and subsequently redissolved nanoparticles. The AFM-based size distribution of the pure GdF_3:**cit** nanoparticles is shown in Figure 1B. Note that the size distribution suggests that particle sizes vary somewhat uniformly between 10 and 150 nm in diameter. An analysis of dynamic light-scattering measurements gives an effective diameter of 129.3 nm in H_2O (average of 3 measurements), with an experimental error of 8 nm and a size range matching that of the AFM distribution. DLS measurements on samples taken from the reaction mixture show size distributions that are slightly broader on the large particle size, suggesting that some reversible agglomeration occurs during the formation of the nanoparticles. The larger

(19) Palmer, R. J.; Butenhoff, J. L.; Stevens, J. B. *Environ. Res.* **1987**, *43*, 142.
(20) Khaled, A.; Guo, S.; Li, F.; Guo, P. *Nano Lett.* **2005**, *5*, 1797.

particles are also expected to arise from growth formation, rather than particle agglomeration. The observation of slightly larger particle sizes with the pure GdF_3:**cit** particles is consistent with the observation that lanthanide solubilities typically decrease across the lanthanide series and that the synthesis protocol results in slightly larger nanoparticles upon replacing La^{3+} with Gd^{3+}. In fact, this was one of the motivating reasons for doping one of the nanoparticles with La^{3+} (namely, those stabilized with 2-aminoethyl phosphate), because solubility was significantly improved. Note that the choice to dope the AEP-coated nanoparticles (versus the citrate-coated nanoparticles) was arbitrary. Ultimately, control of size and solubility is immensely important to targeting and retention times of nanoparticles in living systems and is currently under further investigation. The dynamic light-scattering experiments, which were performed under aqueous conditions and at concentrations similar to those used in the NMR experiments, allow us to estimate the average particle weights, which are 8.6×10^7 and 1.4×10^9 Da for the 80/20 GdF_3/LaF_3:**AEP** and GdF_3:**cit** nanoparticles, respectively. We have shown that statistical mixtures were obtained from mixtures of LaF_3 and EuF_3, and it is safe to assume that the same is true for the current 80/20 GdF_3/LaF_3:**AEP** system,[16d] on the basis of the fact that Gd^{3+} and Eu^{3+} have nearly identical ionic radii.[21] Nevertheless, energy-dispersive X-ray analysis was done on GdF_3/LaF_3:**AEP** nanoparticles, showing a Gd^{3+}:La^{3+} ratio of 79:21 (absolute error is ~1−2%), in perfect agreement with the ratio used in the synthesis. The detection of phosphorus is consistent with the presence of AEP. The Ln^{3+}:F^- ratio is 2.2, which is significantly below the theoretical value of 3 for pure LnF_3. There are two reasons for this. The first is that overall negatively charged ligands are on the surface, which necessitates the presence of excess Ln^{3+} ions. The second reason is that EDX has a probing depth of only a few nanometers in these materials, thus probing the surface of the nanoparticles more than the center.[22]

Figure 2 depicts the dependence of water (90/10 H_2O/^2H_2O) spin−lattice relaxation rates as a function of increasing mass concentrations of each of the two classes of nanoparticles at a Larmor frequency of 600 MHz and temperature of 25 °C. In addition, concentration-dependent water spin−lattice relaxation rates at 63.5 MHz (1.5 T) and 127 MHz (3.0 T) are also presented for the GdF_3:**cit** nanoparticles. On the basis of the slopes, we estimate the mass relaxivities at 600 MHz to be 14.3 and 10.2 s^{-1} $(mg/mL)^{-1}$ for the GdF_3:**cit** and 80/20 GdF_3/LaF_3:**AEP** nanoparticles, respectively. Using the average particle weights determined by the scattering experiments, we can estimate the paramagnetic relaxation rates (per mM nanoparticle). The so-called molar relaxivities turn out to be 2.0×10^7 and 8.8×10^5 s^{-1} mM^{-1} for the GdF_3:**cit** and 80/20 GdF_3/LaF_3:**AEP** nanoparticles, respectively. If we express these relaxivities in terms of the number of Gd^{3+} ions per particle (i.e., 6.3×10^6 Gd^{3+} ions per GdF_3:**cit** particle and 3.25×10^5 Gd^{3+} ions per GdF_3/LaF_3:**AEP** nanoparticle), we obtain ion relaxivities of 3.17 and 2.71 s^{-1} mM^{-1} per Gd^{3+}, respectively. These particle relaxivities compare favorably with those obtained for Gd^{3+} aggregates consisting of dendrimer cores[7,8] or the more recently developed zeolite shells used to sequester Gd^{3+} for MRI studies of the stomach[3] and are slightly smaller than the relaxivities reported for superparamagnetic iron oxide nanoparticles.[23] It is a bit surprising that the above mass relaxivity values of 14.3 and 10.2 s^{-1} $(mg/mL)^{-1}$ exceed that observed for Gd-DTPA[24] and numerous other commercial contrast agents.[25] For example, the relaxivity of Gd:DTPA has been reported as being 2.79 s^{-1} mM^{-1} (i.e., 1.86 s^{-1} $(g/L)^{-1}$) at 1.5 T[26] or 4 s^{-1} mM^{-1} (i.e., 2.7 s^{-1} $(g/L)^{-1}$) at room temperature and 1.5 T in saline,[27] in comparison to our value of 7.4 ± 0.2 s^{-1} $(mg/mL)^{-1}$ for the GdF_3:**cit** nanoparticles.

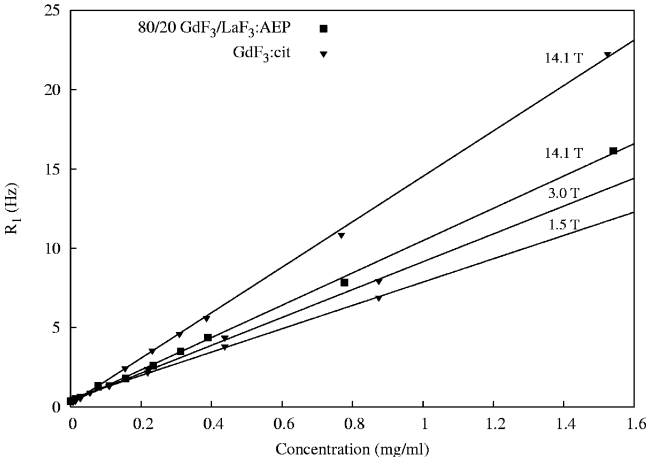

Figure 2. ^1H spin−lattice relaxation rates ($1/T_1$) of H_2O vs mass concentration (mg/mL) of either GdF_3:**cit** (solid triangles) or 80/20 GdF_3/LaF_3:**AEP** (solid squares) nanoparticles in a 90/10 H_2O/D_2O mixture at room temperature and 14.2 T (600 MHz), in addition to lower field strengths (1.5 and 3.0 T). In the case of the GdF_3:**cit** nanoparticles, transverse ($1/T_2$) relaxation rates were found to be within the uncertainty of the estimation of the $1/T_1$ rates at both 1.5 and 3.0 T and are thus not shown.

The high mass relaxivities suggest that the majority of Gd^{3+} ions are contributing to the observed relaxation. However, it is known from electron microscopy studies that the GdF_3 nanoparticles are not porous, and there is very little water exchange to the bulk of the Gd^{3+} ions on the interior. This suggests a high degree of cooperativity, which may arise from a superparamagnetic effect.[28] X-ray measurements have shown that the particles exhibit high crystallinity, which would also support the idea that the particles exhibit superparamagnetism. Furthermore, if only an outer shell of Gd^{3+} ions was responsible for the relaxation, then we would expect to see a dramatically different mass relaxivity between

(21) *CRC Handbook of Chemistry and Physics*, 78th ed.; Lide, D. R., Ed.; CRC Press: Boca Raton, FL, 1997−1998.
(22) A Ln^{3+}:F^- ratio of about 2.8 was observed by EDX on Tm^{3+}-doped LaF_3 nanoparticles with an average size of only 7−10 nm; work submitted.
(23) Lutz, A. M.; Weishaupt, D.; Persohn, E.; Goepfert, K.; Froehlich, J.; Sasse, B.; Gottschalk, J.; Marincek, B.; Kaim, A. H. *Radiology* **2005**, *234*, 765.
(24) D'Arceuil, H. E.; de Crespigny, A. J.; Pelc, L.; Howard, D.; Alley, M.; Seri, S.; Hashiguchi, Y.; Nakatanid, A.; Moseley, M. E. *Magn. Reson. Imag.* **2004**, *22*, 1243.
(25) Livramento, J. B.; Toth, E.; Sour, A.; Borel, A.; Merbach, A. E.; Ruloff, R. *Angew. Chem., Int. Ed.* **2005**, *44*, 1480.
(26) Tilcock, C.; Unger, E.; Cullis, P.; MacDougall, P. *Radiology* **1989**, *171*, 77.
(27) Stanisz, G.; Henkelman, R. *Magn. Reson. Med.* **2000**. *44*, 665.
(28) Wang, Y. J.; Hussain, S. M.; Krestin, G. P. *Eur. Radiol.* **2001**, *11*, 2319.

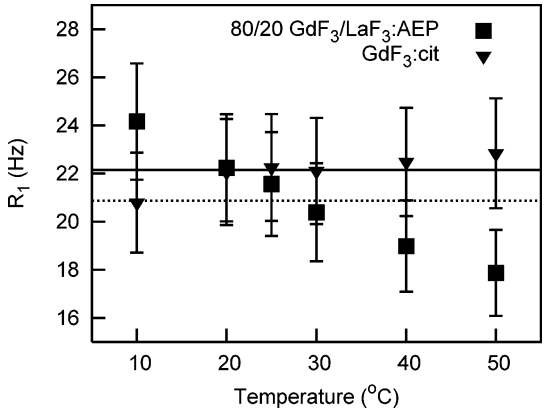

Figure 3. Temperature dependence of the spin−lattice relaxation rates of water for GdF_3:**cit** and the 80/20 GdF_3/LaF_3:**AEP** nanoparticles, at a concentration of 1.53 mg/mL and at 600 MHz ^{1}H Larmor frequency.

the above two nanoparticles, whose sizes differ by more than a factor of 2. Assuming for the moment that only the Gd^{3+} ions in the outer shell, within roughly the radius of water (∼3 Å), contribute to relaxation, we can again estimate the relaxivity per Gd^{3+} ion residing within 3 Å of the nanoparticle surface. Because there are estimated to be 8.8×10^4 and 1.14×10^4 Gd^{3+} ions in the GdF_3:**cit** and GdF_3/LaF_3:**AEP** nanoparticle outer shells, respectively, we obtain relaxivities of 227.3 and 77.2 s^{-1} mM^{-1} per shell Gd^{3+} ion, respectively. Such relaxivities are unheard of, strongly implying that the bulk of the Gd^{3+} ions are contributing to the overall relaxation effects. Finally, we note that T_1 and T_2 experiments of the GdF_3:**cit** revealed mass relaxivities of 7.4 ± 0.2 and 8.4 ± 0.2 s^{-1} $(mg/mL)^{-1}$, respectively, at 1.5 T, whereas identical measurements at 3.0 T revealed respective relaxivities of 8.8 ± 0.2 and 9.4 ± 0.2 s^{-1} $(mg/mL)^{-1}$. Though these relaxivities are lower than those observed at higher fields, they still exceed those of Gd:DTPA and show promise in light of their stability and potential for surface functionalization. We anticipate that further improvements should be possible upon optimizing particle sizes through reaction conditions and nanopore filters (work in progress).

Figure 3 reveals the temperature dependence of the water spin−lattice relaxation rates of both nanoparticles at concentrations of 1.53 and 1.54 mg/mL at 600 MHz. Though relatively constant, the relaxation rates appear to decrease slightly with increasing temperature for the GdF_3:**cit** particles, whereas the GdF_3/LaF_3:**AEP** particles show the opposite trend. Though we cannot explain these differing trends, we speculate that this effect relates to the relative difference in water-exchange rates of water. The relaxivities of both nanoparticles were also measured at additional available field strengths (63.5 MHz and 127, 200, and 500 MHz, respectively). The results, shown in Figure 4, reveal that a pronounced relaxation rate profile with field strength through all relaxation rates has been obtained, which is useful for NMR and imaging purposes.

Figure 5 compares ^{1}H NMR spectra of unlabeled lysozyme with varying amounts of nanoparticle added. Average amide spin−lattice relaxation times were observed to drop from 0.85 to 0.25 s in the presence of only 15 nM 80/20 GdF_3/LaF_3:**AEP** nanoparticles. This corresponds to an average paramagnetic rate of 2.5 s^{-1} for the amide protons of

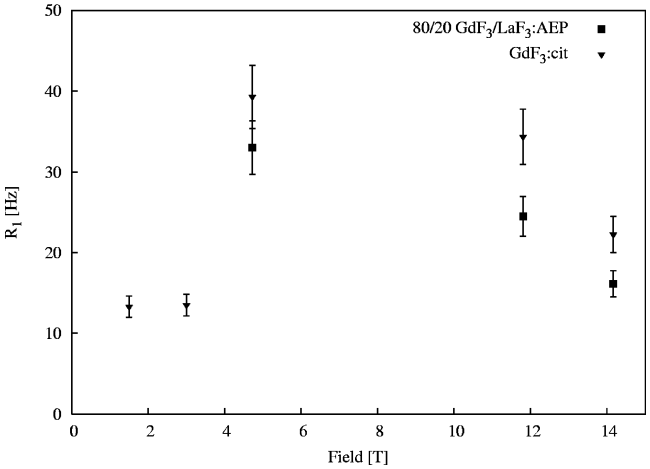

Figure 4. Field dependence of the spin−lattice relaxation rates of water for GdF_3:**cit** and the 80/20 GdF_3/LaF_3:**AEP** nanoparticles, at a concentration of 1.5 mg/mL and at 20 °C.

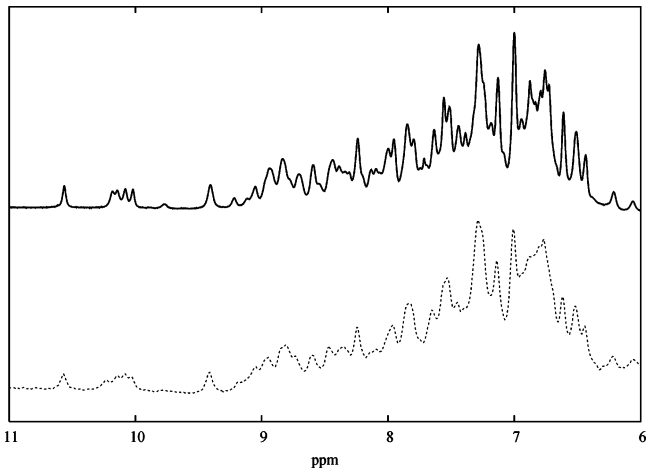

Figure 5. ^{1}H NMR spectrum at 600 MHz of 1 mM lysozyme in a 90/10 buffered solution containing no paramagnetic additives (solid line) and one containing 10 nM 80/20 GdF_3/LaF_3:**AEP** nanoparticles (dotted line). All spectra were recorded using a WATERGATE solvent-suppression sequence at a temperature of 25 °C.

lysozyme. Because of the positive net charge of the protein, the positively charged nanoparticles were chosen to minimize direct interactions between particles and the protein. A similar study was also performed with a small molecule (caffeine), wherein the paramagnetic contribution to ^{1}H spin−lattice relaxation was between 3 and 5 s^{-1} at 12 nM GdF_3:**cit** nanoparticle concentrations. In both cases, the absence of chemical-shift perturbations suggests that the particles are not strongly interacting with the solute molecules of interest and that relaxation is mediated principally via the solvent.

Conclusions

In conclusion, a paramagnetic nanoparticle additive consisting of a GdF_3 core or a GdF_3 and LaF_3 mixed core has been synthesized and rendered highly water soluble through the coordination of surface ligands on the surface. Relaxivities at 600 MHz are such that around 10−15 nM concentrations of nanoparticles, water spin−lattice relaxation times drop to around 125 ms, making them useful for decreasing repetition times in studies of proteins with very long relaxation times. The lack of direct interaction between

nanoparticle and solute and the ease with which the nanoparticles can be removed from an NMR sample through centrifugation suggest that these nanoparticles should be useful as relaxation agents in NMR studies.

Key advantages observed for the nanoparticles as relaxation agents in NMR include the following: (1) high solubility in a range of solvents, (2) high relaxivity over a range of temperature and field strength, without undue line broadening, (3) minimal binding to the solute molecule or macromolecule of interest because of low nanoparticle concentrations and functionalized surfaces with appropriate charge, (4) lack of leaching of ions over considerable periods of time, and (5) ease of removal of nanoparticles by ultracentrifugation, or via a specific matrix such as avidin, in combination with biotinylated beads. In addition, there are advantages anticipated for the nanoparticles, which have the greatest promise in MRI. The mass relaxivities ranged between 7.4 and 9.4 s^{-1} $(mg/mL)^{-1}$ for the GdF_3:**cit** nanoparticles at 1.5 and 3.0 T, which bodes well for MRI applications. In addition, the nanoparticles can readily be functionalized with a multitude of groups. We have demonstrated that these particles can be functionalized with citrate groups, amino groups, and biotin.[29] Unlike dendrimers, zeolites, polypeptides, etc., where multiple ligands are problematic, the lanthanide trifluoride nanoparticles can easily be functionalized (simultaneously) with a multitude of groups. This is much more important in MRI because multiple groups could be envisaged in controlling solubility and retention in specific tissues. Though toxicity studies have yet to be performed, the lack of Gd^{3+} ion leaching, many possibilities for surface functionalization, and possibilities for control of particle size via nanopore filters and synthesis optimization bodes well for potential clinical applications.

Acknowledgment. R.S.P. gratefully acknowledges the American Chemical Society (PRF AC Grant 376620) and the Natural Sciences and Engineering Research Council of Canada (NSERC) for generous funding support. F.v.V. would like to acknowledge the generous funding received from the National Research and Engineering Council (NSERC), the Canada Foundation for Innovation (CFI), and the British Columbia Knowledge Development Fund (BCKDF). We are also grateful to Professor Eugenia Kumacheva and Dr. Alla Petukhova in the Department of Chemistry at the University of Toronto for their assistance in the zeta potential measurements.

CM052299W

(29) (a) Diamente, P. R.; van Veggel, F. C. J. M. *J. Fluoresc.* **2005**, *15*, 543. (b) Diamente, P. R.; Burke, R. D.; van Veggel, F. C. J. M. *Langmuir* **2006**, *22*, 1782.